A COMPARISON OF SURFACE PREPARATION TECHNIQUES FOR WIND TURBINE FIELD REPAIRS

Ariel F. Lusty, Douglas S. Cairns, David A. Miller, Daniel D. Samborsky
Montana State University
Bozeman, MT 59717

ABSTRACT

Wind turbine service lifetimes can exceed 20 years. This extreme operational demand necessitates reliable and consistent field repairs. However, the effects of current wind turbine field repair surface preparation techniques are not well-documented and are thus not well-understood. This leads to reliance on technician experience rather than scientific data for repair procedures, which causes variability in the quality of repairs. Solvent wiping is a common procedure for contaminant removal after damaged material is removed from a wind turbine blade, but it was unknown if solvent wiping reduces the surface energy and consequently the likelihood of a durable repair. The goal of this study was to quantify the effects various surface preparation techniques have on the overall strength and reliability of wind turbine repairs. Type of reagent-grade solvent, fiber direction, matrix, and adhesive were varied for contact angle and lap shear testing. It was found that the type of solvent used affects neither the surface energy nor the maximum lap shear stress, but the fiber direction and matrix-adhesive combinations significantly affected maximum lap shear stress values.

1. INTRODUCTION

Fixing structural damage is of utmost priority for owners and operators of wind turbines. Structural damage is typically from manufacturing defects, but may include in-service damage from mechanical fatigue, bird collisions, or lightning strikes. Damage that inhibits a wind turbine from efficiently harvesting energy should be repaired if the repair does not exceed the cost of blade replacement or if the procedure is economically viable for other reasons. The goal of any repair is to return the structure to its original strength, stiffness, shape, and surface finish [1]. The most common and preferred structural wind turbine blade repair method is the scarf repair due to the need to restore strength, avoid load concentration and eccentricities, and maintain aerodynamic efficiency.

Regardless of the repair design, contamination will be present before, during, and after damage removal. A commonly used technique for contaminant removal involves wiping a surface with reagent grade solvents to remove contamination, and wiping again with a dry cloth to remove the solvent before it evaporates. It is essential to ensure that the solvent being used is capable of dissolving the contaminant without further damaging the composite structure [2]. If the use of solvents damages the surface of the composite structure, bond strengths and repair durability could be compromised. Consequently, contact angle and lap shear testing were conducted to investigate the effects of solvents on composite bond strengths.

Contact angle testing can be used to calculate surface energy, which is the work spent in forming a unit area of a solid surface. Contact angle testing involves the placement of a water droplet on a

Copyright 2020. Used by the Society of the Advancement of Material and Process Engineering with permission.

surface and measuring the resultant angle the droplet makes with the surface. Low contact angle values correspond with hydrophilicity, high wettability, and higher surface energy. Alternatively, high contact angles indicate hydrophobicity, low wettability and lower surface energy [3]. Additionally, low surface energy has been shown to result in more adhesive failure, and high surface energy will typically result in more cohesive failure [4].

Vacuum assisted resin transfer molding (VARTM) was used to manufacture glass fiber reinforced polymer (GFRP) composite substrates. Profilometry was used to examine differences in substrate surfaces after manufacturing as well as after sanding. Sessile drop contact angle testing was conducted after composite samples were sanded and wiped with reagent grade solvents including acetone, methyl ethyl ketone (MEK), methyl isobutyl ketone (MIBK), or isopropyl alcohol (ISP), as these are commonly used solvents in composite repairs [1]. Contact angle testing was also conducted on plasma-treated specimens, as this is a common surface treatment method to increase surface energy [5]. The contact angle decreased significantly for plasma-treated specimens.

In addition to contact angle testing, lap shear testing using two different adhesives was used to compare the effects of wiping substrate surfaces with different solvents on the resulting bond strengths. It is important to note that lap shear testing does not produce true ultimate stress because the stress distribution in the adhesive is not uniform over the bond area [6]. Additionally, the stiffness of adherends influences peel stress concentrations at the end of the joint in lap shear testing. Increasing the modulus or thickness of adherends will lead to an increase in apparent strength of the bond. Nevertheless, lap shear data does have value from a comparative standpoint and can be used to check the effectiveness of different surface preparations [7]. In addition to differences in lap shear strengths, adhesive failure modes were visually examined and photographed. Dillingham demonstrated using double cantilever beam (DCB) testing that cohesive failure corresponded with higher mode I fracture toughness values, and adhesive failure corresponded with lower mode I fracture toughness values [4]. Similarly, there appears to be a correlation between failure modes and maximum lap shear stresses among lap shear results in this study.

If a particular solvent had deleterious effects on bond strength more than another, it would be reflected in differences in lap shear strengths and adhesive failure modes. Overall, the type of solvent used affected neither the contact angle nor the maximum lap shear stress, but the fiber direction and matrix-adhesive combinations significantly affected maximum lap shear stress values due to their differences in thicknesses and moduli.

2. MATERIALS

Materials were selected to replicate the surfaces that would be encountered in a wind turbine blade field repair. Wind turbine blades are typically made using sandwich composites, which consist of foam or balsa cores sandwiched between glass fiber reinforced polymer face sheets as shown in Figure 1. The core adds stiffness and increases buckling resistance while maintaining a high strength to weight ratio at a low cost.

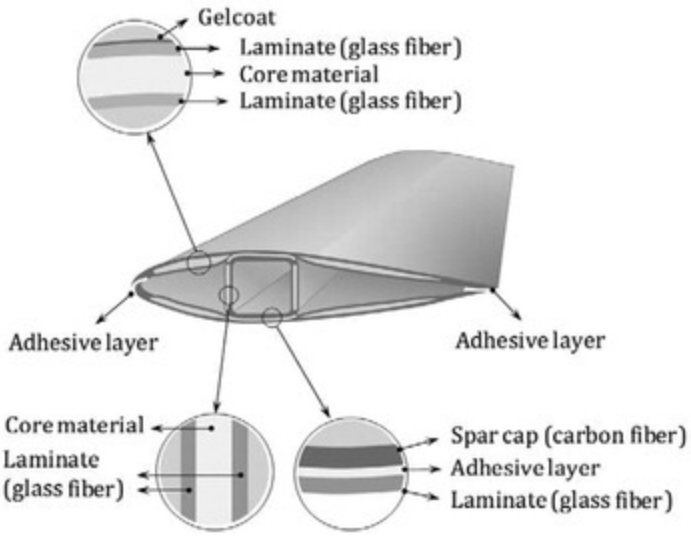


Figure 1. Typical cross-section of a wind turbine blade [8].

Face sheets are often manufactured using both 0° and ±45° glass fibers, with either an epoxy or a vinyl ester matrix. Accordingly, VARTM was used to make $[0]_4$ epoxy, $[45]_6$ epoxy, $[45]_6$ vinyl ester, and $[0]_4$ vinyl ester composites for contact angle and lap shear testing. Unidirectional Vectorply E-LT-2900 fabric was used for the $[0]_4$ layups, and ±45° PPG D810 fabric was used for $[45]_6$ layups. Hexion Epikote MGS RIMR 135/ Epicure MGS RIMH 1366 epoxy was used for the epoxy composites, as this is a commonly used matrix for wind turbine blade manufacturing. Fibreglast 1110 vinyl ester resin was used for vinyl ester composites and was selected for its low viscosity, which is appropriate for VARTM manufacturing.

Polyester peel ply was used between the layup and the vacuum bag during the VARTM manufacturing process. The top of the layup, or where the layup was in contact with the peel ply will be considered as the "rough side" in Table 1. The "rough side" of the laminate obtains its roughness from the textured indentation of the peel ply. The "smooth side" of the laminate is where the layup was in contact with the caul plate. Loctite Frekote 770-NC mold release was used to ensure the laminate would be able to be removed from the caul plate. Furthermore, sanding samples not only energized the surfaces but also removed mold release from samples. To ensure more surface regularity, the "smooth side" of laminates were used for all contact angle and lap shear testing.

Two adhesives were compared in lap shear testing: Huntsman Araldite 2051 and Loctite EA 9396 Aero. Huntsman Araldite 2051 is a two component, toughened methacrylate general purpose adhesive that cures after 15 minutes at room temperature. No post-cure was used for the Huntsman Araldite 2051. Loctite EA 9396 Aero is a two-component, low viscosity room temperature curing adhesive system. Loctite EA 9396 Aero adhesives were post-cured at 66°C for one hour.

Wypall X60 cloths were used for solvent wiping. These cloths were selected for their low lint content and lack of adhesive binders, both features that will decrease the likelihood of contamination and residues being left on a surface when used.

3. EXPERIMENTATION

3.1 Profilometry Testing

Profilometry was conducted to examine differences in the rough and smooth sides of samples as well as the consistency in sanding. The roughness average (R_a) was found using a Mitutoyo SJ-201 profilometer for the sanding methods that were used for contact angle and lap shear testing.

3.2 Solvent Wipe Contact Angle Tests

Sessile drop contact angle testing was conducted after samples were sanded and wiped with solvents. A diagram of a typical sessile-drop contact angle test depicting the three interfacial tension forces is illustrated in Figure 2.

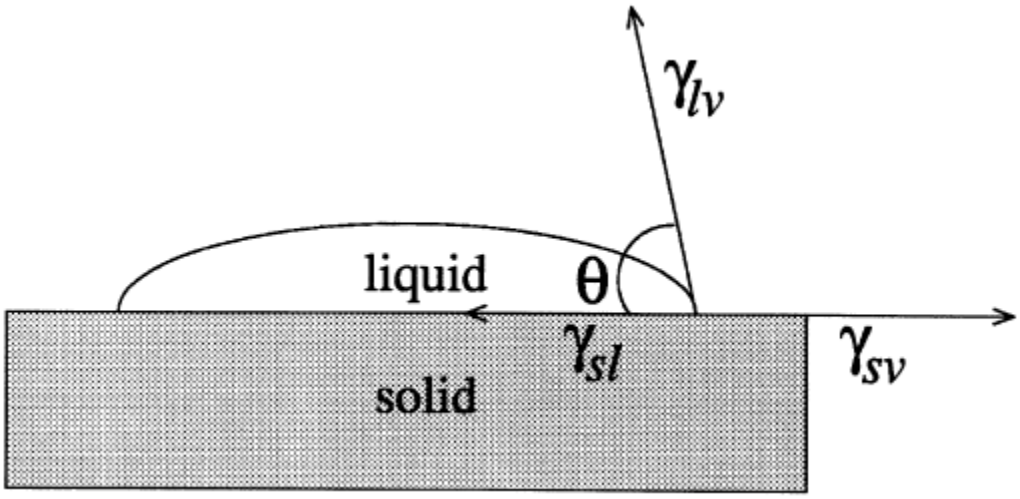


Figure 2. Schematic of a sessile-drop contact angle system at equilibrium [9]. The four variables $\theta, \gamma_{sl}, \gamma_{lv}$, and γ_{sv} are defined as contact angle and interfacial tensions between solid and liquid, between liquid and vapor, and between solid and vapor, respectively [3].

For contact angle testing, samples were first wet sanded using Federation of European Producers of Abrasives (FEPA) 1000 grit sandpaper, then wiped with a dry cloth to remove water. The water break test was used to ensure mold release was removed from composite surfaces [10]. Next, the samples were wiped with another cloth that had been saturated with either distilled water, reagent-grade ISP, acetone, MIBK, or MEK. Then, samples were wiped with a dry cloth. Six contact angle tests were conducted for each sample in the locations illustrated in Figure 3.

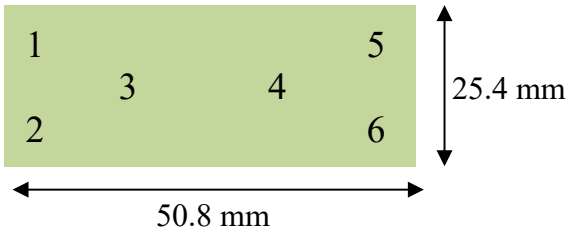


Figure 3. The six locations of contact angle test droplets on a 25.4 x 50.8 mm^2 composite surface.

Contact angle testing was conducted immediately after solvent wiping. A 1 µL droplet of MilliQ 0.2 µm water was formed at the tip of the needle. Next, the substrate was slowly brought up to

the droplet. Once the droplet contacted the surface, the substrate was lowered. The contact angle decreases linearly with time after a water droplet is placed on a surface. Conclusions from preliminary testing demonstrated that water droplets would stabilize, but not completely evaporate, after approximately 10 seconds. Thus, after the droplet was on the composite surface for 10 seconds, an image was captured using VCA Optima software. Contact angles were also measured using VCA Optima.

3.3 Plasma Contact Angle Tests

Specimens cut from the same composite plates as the solvent wipe contact angle tests were shipped to Enercon Industries Corporation for plasma treatments, followed immediately by contact angle testing. Dimensions in Figure 3 were used. Specimens were sanded with FEPA 1000 grit sandpaper prior to shipment to remove mold release. Two areas on each sample were contact angle tested before and after being treated by two surface treatment types: a blown ion treatment and flame treatment. Line speed was run at 30.5 cm per minute for both blown ion and flame treatments. The output used for the blown ion treatment was at 0.5 kW, and the output for the flame burner was 200 liters per minute (LPM). The distance between the blown ion treatment and the sample was 6.35 mm, and the distance between the flame treatment and the sample was 50.8 mm.

3.4 Lap Shear Tests

Instead of the FEPA 1000 sand grit that was used for contact angle testing, FEPA 320 grit sandpaper was used to promote adhesion for lap shear testing. Solvent wipe techniques identical to those used in contact angle testing were used prior to adhesive bonding. Wire with a 0.33 mm diameter was used as spacers, and weights were used to reduce variation in adhesive thicknesses. The maximum lap shear stress is reported as the failure stress in the adhesive, which is found by dividing the failure load by the bond area. The $[45]_6$ laminates were tested at 0.5 in/min load rate to minimize creep, and $[0]_4$ laminates were tested at 0.05 in/min load rate [11]. No significant differences in maximum lap shear stress were found between the two load rates.

4. RESULTS

4.1 Profilometry Results

Results from profilometry tests are shown in Table 1 below.

Table 1. Average surface roughness (μm) and standard deviations of specimens subjected to several surface treatments. Two measurements were made for each tabulated value.

Substrate	Unsanded smooth side	Unsanded Rough Side	320 Grit Sanded Smooth Side	1000 Grit Sanded Smooth Side
$[0]_4$ Epoxy	0.460 ± 0.089	7.407 ± 0.483	0.818 ± 0.030	0.417 ± 0.168
$[45]_6$ Epoxy	0.353 ± 0.033	8.814 ± 1.173	0.815 ± 0.069	0.259 ± 0.069
$[0]_4$ Vinyl Ester	0.927 ± 0.292	9.058 ± 1.168	0.610 ± 0.229	0.335 ± 0.102
$[45]_6$ Vinyl Ester	0.475 ± 0.003	8.735 ± 2.690	0.815 ± 0.107	0.191 ± 0.020

As expected, samples that were sanded with 320 grit sandpaper had higher R_a values than samples sanded with 1000 grit sandpaper. The rough side had the highest R_a values from the

rough indentation left after peel ply removal. Standard deviations remained about the same between sanded and unsanded smooth-sided samples.

4.2 Solvent Wipe Contact Angle Results

Results for contact angle testing after wiping with solvents are summarized in Table 2. The "unprepared" treated samples were neither sanded nor solvent wiped, and still had mold release on these surfaces. The "dry wipe" treated samples were wet sanded and wiped with dry cloths before contact angle testing.

Table 2. Average contact angle (degrees) for each surface treatment.

Treatment	$[0]_4$ Epoxy	$[45]_6$ Epoxy	$[0]_4$ Vinyl Ester	$[45]_6$ Vinyl Ester
Unprepared	87.7 ± 3.5	73.4 ± 5.0	87.8 ± 9.6	70.6 ± 12.8
Dry Wipe	64.3 ± 5.4	66.8 ± 9.7	67.1 ± 6.8	67.6 ± 6.3
Distilled Water	56.5 ± 5.9	79.0 ± 2.1	59.5 ± 9.9	82.1 ± 5.6
ISP	59.4 ± 5.4	70.2 ± 6.4	65.0 ± 9.1	72.0 ± 6.7
Acetone	54.5 ± 7.2	73.0 ± 2.6	67.3 ± 9.4	68.1 ± 3.7
MIBK	62.3 ± 6.1	58.7 ± 6.4	61.1 ± 5.2	71.8 ± 3.7
MEK	62.4 ± 7.3	65.5 ± 8.5	60.9 ± 8.9	68.3 ± 5.8

The contact angle was not significantly altered by wiping samples' surfaces with solvents. However, removing mold release through sanding is crucial to decreasing the contact angle, as shown in the drops in contact angle between "unprepared" and solvent wiped samples in the $[0]_4$ epoxy and vinyl ester columns. Variation in contact angle results among sanded samples may be in part due to variations in fiber exposure.

4.3 Plasma Treatment Contact Angle Results

Contact angles across all solvent-wiped specimens were fairly high, indicating poor wettability and poor adhesion. To decrease contact angle, samples were plasma treated followed by contact angle testing.

Table 3. Average contact angles and standard deviations on composite surfaces before and after blown ion treatment.

Treatment	$[0]_4$ Epoxy	$[45]_6$ Epoxy	$[0]_4$ Vinyl Ester	$[45]_6$ Vinyl Ester
Initial (before blown ion treatment)	73.5 ± 0.2	71.1 ± 0.7	75.0 ± 3.7	70.4 ± 3.7
After blown ion treatment	30.2 ± 2.2	30.6 ± 2.3	16.2 ± 0.0	22.9 ± 0.8

Across all composite surface types in Table 3, there was a 66% drop between the average contact angles before and after blown ion treatment.

Table 4. Average contact angles and standard deviations on composite surfaces before and after flame treatment.

Treatment	$[0]_4$ Epoxy	$[45]_6$ Epoxy	$[0]_4$ Vinyl Ester	$[45]_6$ Vinyl Ester
Initial (before flame treatment)	70.2 ± 0.1	78.5 ± 2.5	63.5 ± 0.2	77.7 ± 1.3
After flame treatment	25.8 ± 0.4	28.9 ± 0.9	15.9 ± 0.4	18.8 ± 2.5

Across all composite surface types in Table 4, there was a 69% drop between the average contact angles before and after flame treatment. Overall, contact angle dropped significantly between initial and plasma treated composite surfaces for both blown ion and flame treatments.

4.4 Lap Shear Results

The moduli of the $[0]_4$ and $[45]_6$ adherends were 39.4 and 13.3 GPa, respectively. Lap shear test results for the Huntsman Araldite 2051 adhesive are shown in Table 5 and 6 in addition to Figures 4 and 5. Lap shear test results for the Loctite EA 9396 Aero adhesive are shown in Tables 7 and 8 as well as Figure 6.

Table 5. Average maximum lap shear stress (MPa) and standard deviations for 658 ± 19 mm^2 average bond area of Huntsman Araldite 2051.

Surface Treatment	$[0]_4$ Epoxy	$[45]_6$ Epoxy	$[0]_4$ Vinyl Ester	$[45]_6$ Vinyl Ester
Sanded	14.89 ± 0.77	6.89 ± 0.29	22.61 ± 1.56	7.69 ± 0.63
ISP	14.52 ± 0.55	7.31 ± 0.58	22.17 ± 1.45	6.57 ± 0.93
Acetone	13.67 ± 2.33	6.88 ± 0.78	22.80 ± 0.46	8.48 ± 0.48
MIBK	14.13 ± 1.38	6.99 ± 0.94	22.75 ± 1.65	7.96 ± 0.13
MEK	13.49 ± 2.14	6.83 ± 1.21	23.63 ± 0.86	8.07 ± 0.38

The $[0]_4$ vinyl ester specimens had higher maximum lap shear stresses than the $[0]_4$ epoxy specimens. The epoxy and vinyl ester $[45]_6$ specimens all had around the same maximum lap shear stresses. There were no significant differences in maximum lap shear stresses from different solvents.

Table 6. Average adhesive and adherend thicknesses, adhesive and adherend standard deviations, and lap shear failure modes for Huntsman Araldite 2051 adhesive.

Substrate	Adhesive thickness (mm)	Adherend thickness (mm)	Primary Failure Mode
$[0]_4$ Epoxy	0.49 ± 0.14	3.21 ± 0.07	Adhesive failure
$[45]_6$ Epoxy	0.46 ± 0.18	2.09 ± 0.06	Fiber-tear failure
$[0]_4$ Vinyl Ester	0.33 ± 0.15	3.12 ± 0.07	Adhesive failure
$[45]_6$ Vinyl Ester	0.57 ± 0.20	2.24 ± 0.06	Fiber-tear failure

Adhesive thickness was generally higher than the diameter of the spacing wire used, likely from the high viscosity of the adhesive. The unidirectional specimens were about 1 mm thicker than the cross-ply specimens, which is the likely source of differences among lap shear results among different substrates along with differences in adherend moduli. The $[0]_4$ specimens resulted in mostly adhesive failure, and the $[45]_6$ specimens had mostly fiber-tear failure. Figure 4 shows the most common failure modes for each substrate. Besides specimens wiped with MEK, failure modes among solvent wipes did not vary significantly.

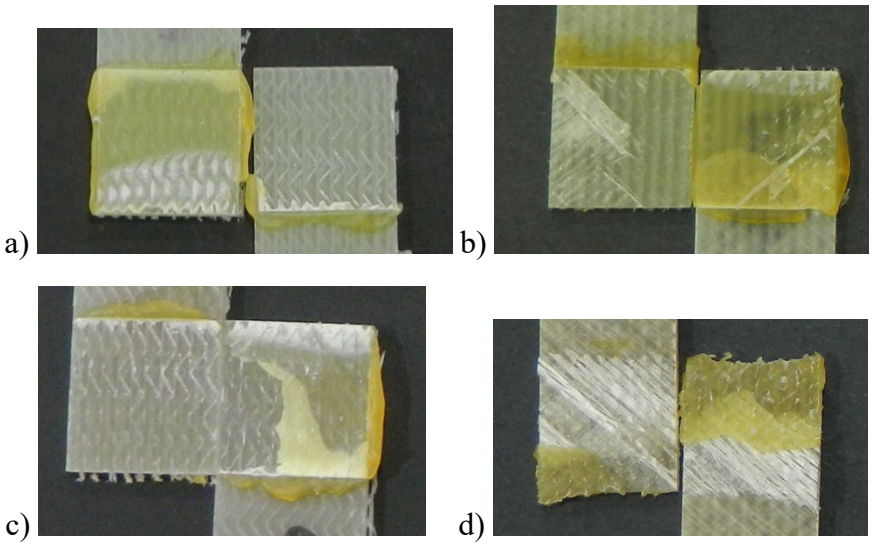


Figure 4. Photographs of the primary failure modes for each substrate: a) $[0]_4$ epoxy adhesive fracture surface (ISP wipe) with adhesive failure mode; b) $[45]_6$ epoxy adhesive fracture surface (MIBK wipe) with fiber-tear failure mode; c) $[0]_4$ vinyl ester fracture surface (ISP wipe) with adhesive failure mode; d) $[45]_6$ vinyl ester adhesive fracture surface (MEK wipe) with fiber-tear failure mode.

Compared to Figure 4 c, Figure 5 shows more cohesive failure.

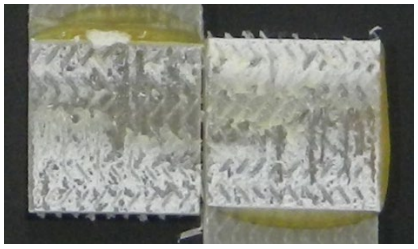


Figure 5. Primary failure mode for $[0]_4$ vinyl ester specimens wiped with MEK.

Although most $[0]_4$ vinyl ester specimens exhibited adhesive failure modes, those wiped with MEK exhibited the most instances of cohesive failure modes but did not have significantly higher maximum lap shear stresses. Overall, though, the layup-matrix combinations had the most differences in resulting maximum lap shear strengths. The $[0]_4$ specimens resulted in higher maximum lap shear strengths and $[45]_6$ layups resulted in the lowest maximum lap shear

strengths. The $[45]_6$ specimens failed at lower ultimate tensile stresses than the $[0]_4$ specimens due to their higher susceptibility to bending in tension.

Table 7. Average maximum shear stress (MPa) for 658 ± 16 mm^2 average bond area of Loctite EA 9396 Aero Adhesive.

Surface Treatment	$[0]_4$ Epoxy	$[45]_6$ Epoxy	$[0]_4$ Vinyl Ester	$[45]_6$ Vinyl Ester
Sanded	13.84 ± 0.82	8.12 ± 0.47	5.81 ± 0.26	4.62 ± 0.50
ISP	13.05 ± 0.91	8.23 ± 0.30	6.56 ± 0.48	5.67 ± 0.32
Acetone	12.54 ± 0.27	8.16 ± 0.19	5.40 ± 0.28	4.96 ± 0.62
MIBK	13.39 ± 0.72	8.21 ± 0.14	5.63 ± 0.61	4.94 ± 0.48
MEK	12.62 ± 0.60	8.24 ± 0.11	5.81 ± 0.47	4.77 ± 0.34

When using the Loctite EA 9396 Aero adhesive, the $[0]_4$ epoxy specimens had the highest maximum lap shear stresses, and the vinyl ester specimens had the lowest maximum lap shear stresses.

Table 8. Average adhesive and adherend thicknesses and lap shear failure modes for epoxy specimens with Loctite EA 9396 Aero Adhesive.

Substrate	Adhesive thickness (mm)	Adherend thickness (mm)	Primary Failure Mode
$[0]_4$ Epoxy	0.15 ± 0.12	3.14 ± 0.03	Cohesive failure
$[45]_6$ Epoxy	0.11 ± 0.08	2.29 ± 0.04	Fiber-tear failure
$[0]_4$ Vinyl Ester	0.13 ± 0.13	3.16 ± 0.06	Adhesive failure
$[45]_6$ Vinyl Ester	0.20 ± 0.18	2.39 ± 0.04	Fiber-tear failure

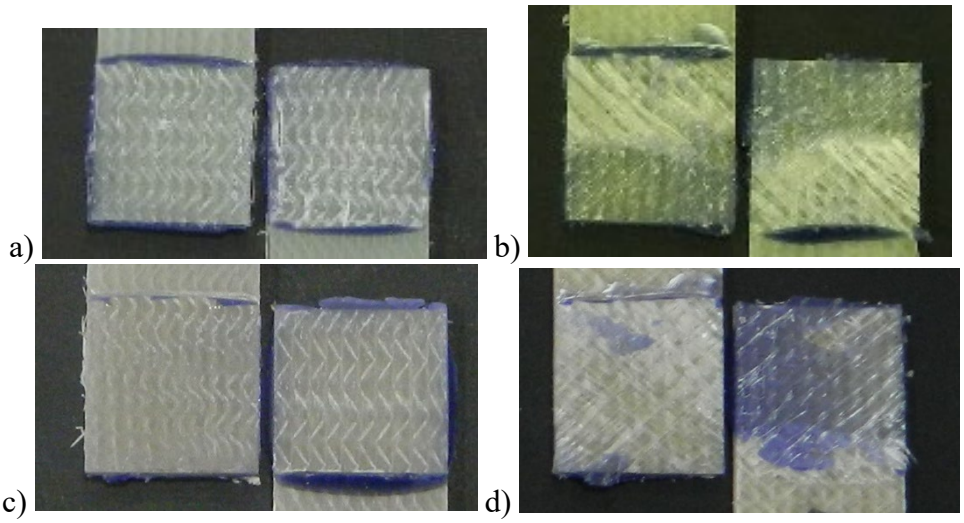


Figure 6. Photographs of the primary failure modes for each substrate: a) $[0]_4$ epoxy adhesive fracture surface (ISP wipe) with cohesive failure mode; b) $[45]_6$ epoxy adhesive fracture surface (MEK wipe) with fiber-tear failure mode; c) $[0]_4$ vinyl ester fracture surface (acetone wipe) with

adhesive failure mode; d) $[45]_6$ vinyl ester adhesive fracture surface (MIBK wipe) with fiber-tear failure mode.

The $[0]_4$ epoxy specimens resulted in mostly cohesive failure, while the $[0]_4$ vinyl ester specimens resulted in mostly adhesive failure. Typically, substrates that have similar molecular structures as the adhesives that are used with them result in higher bond strengths. Since the Loctite EA 9396 Aero adhesive is an epoxy, the $[0]_4$ epoxy specimens likely had the highest bond strengths and optimal failure modes because the epoxy substrates had a similar molecular structure as the epoxy adhesive.

5. CONCLUSIONS

Generally, wiping a composite substrate with either distilled water, ISP, Acetone, MIBK, or MEK neither significantly affects the resulting water contact angle, nor the lap shear strength. Unidirectional vinyl ester specimens resulted in more cohesive failure when wiped with MEK than for those wiped with other solvents, but maximum lap shear strengths were not significantly higher for these specimens. Even so, the causes for the increases in cohesive failure modes for the MEK-wiped specimens merit further investigation. Consequently, DCB and end-notch flexure (ENF) testing will be conducted to examine effects of solvent wiping on modes I and mode II fracture toughness. Since lap shear testing does not give the actual adhesive shear stress, DCB and ENF testing will also provide data that may be used in modeling software such as ABAQUS.

In addition to DCB and ENF testing, chemical testing such as Fourier transform infrared (FTIR) spectroscopy and energy-dispersive X-ray (EDX) spectroscopy will be used to further examine spectral differences in surfaces of composite specimens wiped with solvents. In addition to more mechanical and chemical testing and analysis of solvent effects on the composite surfaces, equally important testing of the effects of common contaminants on repair bond strengths and durability will be executed. Some common contaminants include hydraulic fluid and composite dust, and the effectiveness of each solvent on the removal of these contaminants will be studied.

Contact angle testing demonstrated not only the importance of removing mold release from composites prior to bonding, but also variation in contact angles among sanded samples. This may be due to variation from sanding techniques and also variation in fiber exposure. Plasma treatment delivered promising results for decreasing contact angle, but may be challenging to implicate into wind turbine field repairs due to already-present challenges with wind turbine blade accessibility. Furthermore, the effectiveness of applying sizing to the surface of a composite in increasing resultant repair bond strengths will be examined.

Differences observed when testing different lap shear substrates were mostly due to differences in adherend thicknesses and moduli rather than the type of solvent used. Adhesive-matrix combination also had a significant effect on the maximum lap shear stresses. The Huntsman Araldite 2051 adhesive resulted in 45% higher maximum lap shear stresses with vinyl ester specimens than epoxy specimens. The Loctite EA 9396 Aero adhesive resulted in 96% higher maximum lap shear stresses with epoxy specimens than with vinyl ester specimens, and the Huntsman Araldite 2051 adhesive resulted in 61% higher maximum lap shear strengths than the Loctite EA 9396 Aero adhesive particularly when used with the $[0]_4$ vinyl ester specimens.

Additional adhesives such as Fibreglast 1101 Epoxy Paste Bonding Adhesive and Plexus MA 310 methacrylate adhesive will be used in the future contamination and sizing effect studies.

After additional testing using different adhesives and studying the effects of common contaminants and surface treatments using mechanical and chemical testing methods, procedures will be developed for the evaluation of solvent effects on composite surfaces, the evaluation of the effectiveness of solvents on the removal of common contaminants, and the evaluation of surface treatment effectiveness on increasing repair bond strength and durability. The development of these procedures is crucial to the advancement of wind turbine blade repair technology and thus the extension of wind turbine blade lifetimes.

6. REFERENCES

[1] L. C. Dorworth, "Repairs for Advanced Composite Structures," in *Automotive Composites Conference and Exhibition*, 2013.

[2] L. C. Dorworth, G. L. Gardiner, and G. M. Mellema, *Essentials of Advanced Composite Fabrication and Repair*. Aviation Supplies & Academics, Inc., 2009.

[3] H. Y. Erbil, *Surface Chemistry of Solid and Liquid Interfaces*. Oxford, UK: Blackwell Publishing Ltd, 2006.

[4] R. G. Dillingham and B. R. Oakley, "Surface Energy and Adhesion in Composite–Composite Adhesive Bonds," *J. Adhes.*, vol. 82, no. 4, pp. 407–426, 2006.

[5] D. M. Mattox, "Chapter 2 - Substrate ('Real') Surfaces and Surface Modification," D. M. B. T.-H. of P. V. D. (PVD) P. (Second E. Mattox, Ed. Boston: William Andrew Publishing, 2010, pp. 25–72.

[6] F. C. Campbell, "Manfacturing Processes for Advanced Composites." New York : Elsevier, New York, 2004.

[7] B. Duncan and L. Crocker, "Review of Tests for Adhesion Strength," National Physics Laboratory Materials Centre, Teddington, Middlesex, UK, 2001.

[8] K. B. Katnam, A. J. Comer, D. Roy, L. F. M. da Silva, and T. M. Young, "Composite Repair in Wind Turbine Blades: An Overview," *J. Adhes.*, vol. 91, no. 1–2, pp. 113–139, 2015.

[9] D. Y. Kwok and A. W. Neumann, "Contact Angle Measurement and Contact Angle Interpretation," *Adv. Colloid Interface Sci.*, 1999.

[10] L. J. Hart-Smith, R. W. Ochnsner, and R. L. Radecky, "Surface Preparation of Composites for Adhesive-Bonded Repair," in *Engineered Materials Handbook: Adhesives and Sealants*, ASM International, 1990.

[11] ASTM Standard D5868-01, 2014, "Standard Test Method for Lap Shear Adhesion for Fiber Reinforced Plastic (FRP) Bonding." ASTM International, West Conshohocken, PA, 2014, DOI: 10.1520/D5868-01R14, www.astm.org.